THE JOURNAL OF BIOLOGICAL CHEMISTRY VOL. 286, NO. 42, pp. 36830–36840, October 21, 2011

Quenching in *Arabidopsis thaliana* Mutants Lacking Monomeric Antenna Proteins of Photosystem II*[S]

Received for publication, June 17, 2011, and in revised form, August 11, 2011 Published, JBC Papers in Press, August 15, 2011, DOI 10.1074/jbc.M111.273227

Yuliya Miloslavina[‡§1], Silvia de Bianchi[¶1], Luca Dall'Osto[¶], Roberto Bassi[‖¶], and Alfred R. Holzwarth[‡2]

From the [‡]Max-Planck-Institut für Bioanorganische Chemie, Stiftstraße 34-36, D-45470 Mülheim a.d.Ruhr, Germany, the [§]Institute of Plant Biology, Biological Research Center, Hungarian Academy of Sciences, 6701 Szeged, Hungary, the [¶]Dipartimento di Biotecnologie, Università di Verona, I-37134 Verona, Italy, and the [‖]Institut für Pflanzenwissenschaften-2, Pflanzenwissenschaften, Forschungszentrum Jülich, D-52425 Juelich, Germany

The minor light-harvesting complexes CP24, CP26, and CP29 have been proposed to play a key role in the zeaxanthin (Zx)-dependent high light-induced regulation (NPQ) of excitation energy in higher plants. To characterize the detailed roles of these minor complexes in NPQ and to determine their specific quenching effects we have studied the ultrafast fluorescence kinetics in knockout (ko) mutants koCP26, koCP29, and the double mutant koCP24/CP26. The data provide detailed insight into the quenching processes and the reorganization of the Photosystem (PS) II supercomplex under quenching conditions. All genotypes showed two NPQ quenching sites. Quenching site Q1 is formed by a light-induced functional detachment of parts of the PSII supercomplex and a pronounced quenching of the detached antenna parts. The antenna remaining bound to the PSII core was also quenched substantially in all genotypes under NPQ conditions (quenching site Q2) as compared with the dark-adapted state. The latter quenching was about equally strong in koCP26 and the koCP24/CP26 mutants as in the WT. Q2 quenching was substantially reduced, however, in koCP29 mutants suggesting a key role for CP29 in the total NPQ. The observed quenching effects in the knockout mutants are complicated by the fact that other minor antenna complexes do compensate in part for the lack of the CP24 and/or CP29 complexes. Their lack also causes some LHCII dissociation already in the dark.

Plants use light as the energy source for their metabolism. During the early steps of photosynthesis, solar energy is efficiently absorbed, and excitons are transferred to the photosynthetic reaction centers (RC)[3] by a complex array of pigment-binding proteins, the light-harvesting antenna complexes (LHC), localized at the periphery of each photosystem (PS) (1, 2) (for recent reviews, see Refs. 3 and 4). However, Lhc proteins are not only involved in light harvesting. Rather, they are also acting in photoprotection by multiple mechanisms, including chlorophyll (Chl) singlet (Chl*) energy dissipation, Chl triplet quenching, and scavenging of reactive oxygen species. The antenna system, thus, has a dual function. On the one hand, it harvests photons and extends the cross-section for light absorption under light-limiting conditions. On the other hand, it prevents or limits damage to the photosynthetic apparatus when light is in excess (5, 6). Among the photoprotective mechanisms catalyzed in the PSII antenna system of higher plants, the high energy-dependent quenching of Chl singlet excited states (qE part of NPQ) is essential for protection under variable light conditions (7) by dissipating the excess energy as heat. Triggering of qE occurs upon decrease of the thylakoid lumen pH (7, 8) under conditions when ATPase cannot fully use the proton gradient created across the thylakoid membrane. Low lumenal pH induces the conversion of violaxanthin (Vx) to zeaxanthin (Zx) via the xanthophyll cycle (9–11) and activates the PsbS protein (12, 13). Both events are essential for the full establishment of quenching. Although early proposals suggested PsbS as the quenching site for ^{1}Chl*, it is now widely accepted that the primary quenching event(s) are located within the antenna system of PSII (14) in agreement with the observation of strong down-regulation of NPQ in Chl *b*-less mutants, which retain PsbS and are depleted in Lhcb subunits (15, 16). The Chl *b* containing antenna consists of one copy each per PSII of the three monomeric proteins called CP29 (Lhcb4), CP26 (Lhcb5), and CP24 (Lhcb6) and two to four copies, depending on light conditions during growth, of the major antenna complex, called LHCII. The latter is a heterotrimer of the Lhcb1, Lhcb2, and Lhcb3 subunits in varying combinations (17, 18). The mechanism(s) for qE have been proposed based on the study of quenching in isolated proteins and point either to a major role of the trimeric LHCII (19), or to the direct involvement of monomeric Lhcb proteins CP29, CP26, and CP24 (20–23). In the former proposal LHCII would either undergo an aggregation-induced conformational change assisted or enhanced by Zx, thus allowing for energy transfer quenching by a lutein (19), or the LHCII quenching would be effected by the formation of a Chl-Chl charge transfer state (24, 25). In the second mechanism qE quenching involves Zx, located in the monomeric antenna complexes of PSII. Zx could act as a direct quencher due to transient formation of a Zx^+ radical cation and a Chl^-

* This work was supported by the Marie Curie Initial Training Network "HARVEST" Grant 238017 within the FP7 program of the European Union, Sonderforschungsbereich Grant SFB 663, Heinrich-Heine-Universität Düsseldorf, and the Max-Planck-Institutes Mülheim a.d. Ruhr.

[S] The on-line version of this article (available at http://www.jbc.org) contains supplemental Fig. S1 and Table S1.

[1] Both authors equally contributed to this work.

[2] To whom correspondence should be addressed: Max-Planck-Institut für Bioanorganische Chemie, Stiftstraße 34-36, D-45470 Mülheim a.d.Ruhr, Germany. Fax: 49-0-208-306-3951; E-mail: holzwarth@mpi-muelheim.mpg.de.

[3] The abbreviations used are: RC, reaction center; Chl, chlorophyll; CP, chlorophyll-binding protein; DAS, decay-associated spectra; DCMU, 3-(3′,4′-dichlorophenyl)-1,1-dimethylurea; HL, high light; ko, knockout; LHC, light harvesting complex; NPQ, non-photochemical quenching; ΔpH, transthylakoid proton gradient; PAM, pulse amplitude modulated; PS, photosystem; RP, radical pair; XC, xanthophyll cycle; Zx, zeaxanthin; Vx, violaxanthin; qE, ΔpH-dependent component of NPQ.

radical anion, followed by recombination to the ground state (22). Lutein bound to the monomeric antenna complex Lhcb was also proposed to participate in the catalysis of qE by carotenoid cation formation (26, 27). *In vivo*, elucidation of the functional role of individual Lhcb proteins has been attempted using reverse genetic strategies (28, 29). Recent studies of the koCP24, koCP26 and the double mutant koCP24/CP26 indicated a major role for CP24 in NPQ (29), although later work indicated a decreased pH gradient rather than a lack of quencher species to be responsible for the reduced quenching in koCP24 (30). Furthermore, biochemical analysis coupled with electron microscopy of grana membranes has highlighted the role of membrane protein dynamics, showing that during NPQ the PSII-supercomplex undergoes dissociation and segregation into two domains containing, respectively, C_2S_2 particles, including PSII core, CP29, CP26, and LHCII-S, and a disconnected antenna system composed of CP24 together with LHCII-M and LHCII-L (31).

The quenching activity was studied in intact *Arabidopsis* leaves by ultrafast Chl fluorescence kinetics after establishment of the steady state NPQ under physiological conditions (32). Unlike other methods applied so far, this spectroscopic approach allows to distinguish between two very different quenching situations: (i) the development of a quenching site(s) in the PSII antenna without a decrease of the physical antenna size, and/or (ii) the decrease of the antenna size due to a functional detachment of parts of the PSII antenna. Quenching in the first case specifically increases the non-radiative deactivation rate k_D of the Chl pigments in the antenna and thus decreases the (average) lifetime of the PSII fluorescence without a change in the total amplitude of the PSII components. The second case leads to a decrease in the total amplitude of the PSII-associated lifetimes due to partial antenna detachment (for a full explanation of these qualitative differences, see Holzwarth *et al.* (32)). Concomitantly a new additional fluorescence lifetime component originating from the functionally detached antenna is expected to appear. This detached antenna may be either quenched or not quenched (32). Based on this type of fluorescence lifetime analysis "*in vivo,*" two independent quenching sites, Q1 and Q2, were proposed to be activated during NPQ (32). The Q1 was shown to be located in the major LHCII complex, which is functionally detached from the PSII/RC supercomplex by a mechanism that strictly requires PsbS, but not Zx. Quenching site Q2 was proposed to be located in the antenna complement remaining connected to the PSII core. This quenching is strictly dependent on Zx formation (it is thus absent, *e.g.* in *npq1* plants) (25, 32). A major conclusion from those studies was that the two quenching sites may also involve two different quenching mechanisms: one requiring PsbS activation only, the other requiring Zx formation, operating essentially independently from each other. These two proposed quenching sites do appear to correlate well with the two physical domains of grana demonstrated by electron microscopy to form upon NPQ induction (31).

In the present paper we specifically address the role of the individual monomeric Lhcb proteins in high light-induced quenching. To test the Q2 site quenching model we study by time-resolved fluorescence under quenched and unquenched conditions a set of monomeric antenna knockout mutants. They include a triple mutant koCP29 (koLhcb4.1/Lhcb4.2/koLhcb4.3), which completely lacks CP29 and is affected in the kinetics of NPQ formation, a koCP26, and a double koCP24/CP26 mutant. The results support the two quenching sites model (32) and allow us to determine the main location of the Zx-dependent Q2 site quenching in the C_2S_2 domain of the PSII complex. The Q2 quenching is strongly attenuated or absent in the koCP29 mutant. This data lead us to conclude that during the establishment of NPQ *in vivo* the PSII supercomplex dissociates into two moieties, which segregate into distinct domains of the grana membrane, thus supporting the previously proposed results (31–33). Notably the data also show that antenna proteins disconnected in the dark from the PSII supercomplex by the effect of knockout of monomeric Lhcs, nevertheless, undergo strong quenching upon induction of NPQ, very similar to the antenna complexes disconnected in the WT by light.

EXPERIMENTAL PROCEDURES

Plant Material and Growth Conditions—Arabidopsis thaliana T-DNA insertion mutants (*Columbia* ecotype) SALK_077953, with insertion in the *lhcb6* gene, SALK_014869, with insertion in the *lhcb5* gene, and the double mutant koLhcb5/Lhcb6 were previously selected (30, 34). Triple mutant koCP29 (koLhcb4.1/Lhcb4.2/Lhcb4.3) was isolated as described in Ref. 31. Fully developed leaves of ~4–5-week-old plants were used for the experiments. Pigment-protein analysis, transition electron microscopy, and other detailed study of these knockout mutants (except koCP29) has been recently published (30).

In Vivo Fluorescence and NPQ Measurements—NPQ of chlorophyll fluorescence, photochemical quenching, and PSII yield (Φ_{PSII}) were measured on whole plants at room temperature with a PAM 101 fluorimeter (Walz). Minimum fluorescence (F_0) was measured with a 0.15 μmol m^{-2} s^{-1} beam, F_m was determined with a 1-s light pulse (5000 μmol m^{-2} s^{-1}), and white continuous actinic light (600 μmol m^{-2} s^{-1}) was supplied by a KL1500 halogen lamp (Schott). NPQ was calculated according to the following equation (35): $NPQ = (F_m - F'_m)/F'_m$, where F_m is the maximum chlorophyll fluorescence from dark-adapted leaves and F'_m is the maximum chlorophyll fluorescence under actinic light exposition. Calculation of fluorescence parameters of chlorophyll fluorescence photochemical quenching, Φ_{PSII}, and relative ETR was performed as described previously (36).

Fluorescence induction kinetics was measured with a home-built apparatus. Fluorescence was excited using a green LED with peak emission at 520 nm and detected in the far-red (>700 nm). For the antenna size determination, leaf discs were infiltrated with 3.0×10^{-5} M DCMU and 150 mM sorbitol. Variable fluorescence was induced with a green light of 7 μmol m^{-2} s^{-1}. The time corresponding to two-thirds of the fluorescence rise ($T_{⅔}$) was taken as a measure of the functional antenna size of PSII (37).

Measurement of ΔpH—The kinetics of ΔpH formation across the thylakoid membrane was measured on intact chloroplast using the method of 9-aminoacridine fluorescence quenching

(38). ΔpH build-up was induced by red actinic light, 600 μmol m^{-2} s^{-1} at RT.

Time-resolved Fluorescence Measurements—Fluorescence decays were measured by single photon timing to a high S/N ratio in the 678–734 nm wavelength region, excited at 663 nm. For excitation a synchronously pumped cavity-dumped dye laser system with a mode-locked argon ion laser (Spectra Physics) as a pumping source was used (39, 40). The fluorescence decays were analyzed by global target analysis (32, 41). Detached plant leaves were placed in a rotation cuvette, consisting of two glass plates (diameter of 10 cm) separated by a 1.5-mm spacer, which was also oscillated sideways. Fluorescence was measured in a front face arrangement from the upper side of the leaves. The cuvette was filled with a sucrose solution (0.3 M) (32).

The lifetime measurements were performed at three different conditions as described before (32): (i) unquenched F_0 state fluorescence (open PSII RCs) was measured in complete darkness after dark-adaptation overnight. The laser frequency was 800 kHz, the rotation speed of the cuvette was 1800 rpm with 78 side movements/min. Preliminary checks were done to ensure that all PSII RCs were indeed open. (ii) For measurements at unquenched maximal fluorescence F_m conditions (PSII RCs closed), leaves were cut at the stem and dipped immediately in a 45 μM DCMU solution with the main part of the leaf that was later used for measurement exposed to air. The detached leaves were incubated for 14 h in the DCMU solution in complete darkness (42). For achieving full closure of the PSII RCs during the measurement an additional blue LED light spot of very low intensity (~20 μmol of photons m^{-2} s^{-1}) was applied immediately before detection of the signal. The laser frequency was 4 MHz and the cuvette was rotated at 1300 rpm and swung sideways at 78 movements/min. (iii) Light adaptation for the quenched F_{NPQ} state was carried out using a mixed array plate of red and amber high intensity light-emitting diodes providing 550–600 μmol of photons m^{-2} s^{-1}. Measurements were started after about 30 min of illumination, *i.e.* after stabilization of the NPQ quenching (*cf.* Fig. 1). For closing all PSII RCs under quenched F_{NPQ} conditions an additional blue high intensity LED (~2000 μmol of photons m^{-2} s^{-1}) was focused on a <1 cm diameter spot right before the area where the measuring laser light pulses (1.5-mm diameter spot) were provided. A 4-MHz laser pulse frequency was used and the cuvette was rotated at 1800 rpm and moved at 78 movements/min. Under these conditions the PSII RCs are fully closed.

To measure a full decay-associated spectra (DAS) at one condition about 45–60 min measuring time was needed, depending on the specific condition. For every condition freshly prepared leaves from the same batch were used.

RESULTS

Long Term NPQ Behavior—Data collection for time-resolved measurements under NPQ conditions requires up to 1 h (see above). As a control for the quenching state condition of the sample we thus checked by normal PAM pulse fluorometry the NPQ behavior over this long time range for the genotypes analyzed in this work. This provided the steady state F_0 and F_m values, respectively, in the absence of actinic light and in the presence of a saturating flash, as well as the induction behavior and NPQ value on the long time range (up to 1 h) (Fig. 1). This analysis shows that knockout mutants have important differences in their kinetics and also in the end level of NPQ induction as already previously reported (29–31). This control also shows that the different genotypes all reach quite well defined steady state levels of NPQ after 20–30 min, which is similar for all genotypes (around NPQ = 2). The quenched state was rapidly reversible in all genotypes upon switching off the actinic light.

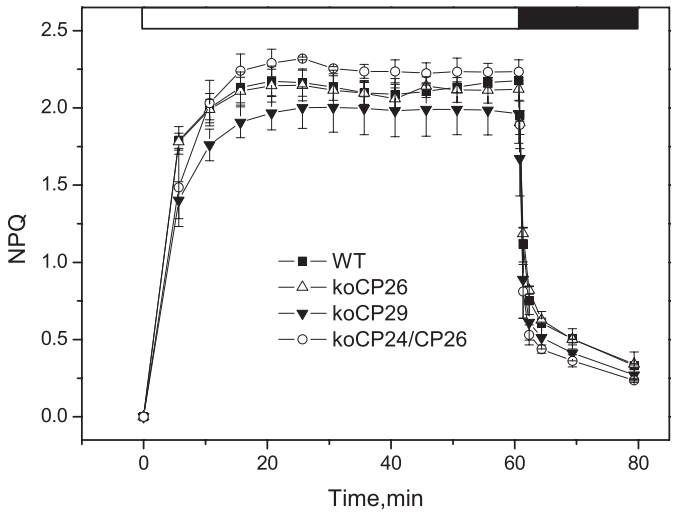

FIGURE 1. **Long-term NPQ analysis of wild-type and antenna mutants.** The kinetics of NPQ induction and relaxation were recorded with a PAM fluorometer in WT and koCP26, koCP29, and koCP24/CP26 mutants. Chl fluorescence was measured in intact, dark-adapted leaves, during 60 min of illumination at 600 μmol m^{-2} s^{-1} followed by 20 min of dark relaxation. Mean values (±S.D.) of three to five independent measurements are shown.

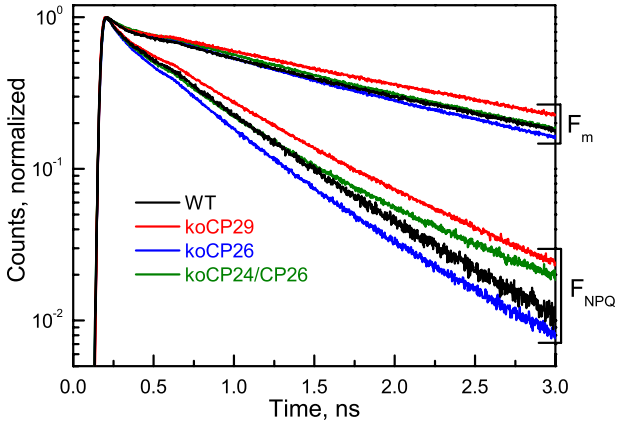

FIGURE 2. **Normalized fluorescence decays (on a semilogarithmic scale) detected at 686 nm for WT and knockout mutants of intact leaves of *A. thaliana*.** koCP26, koCP29, and koCP24/CP26 in the quenched (light-adapted) F_{NPQ} and the unquenched (DCMU-treated) F_m conditions, both with fully closed PSII RCs.

Fluorescence Decay—Fig. 2 shows original fluorescence decays measured by single photon counting at 686 nm on intact leaves of the knockout mutants: koCP26, koCP24/CP26, and koCP29. For each genotype two decays are presented, respectively, for the unquenched dark-adapted state (F_m; PSII RCs closed) and the quenched light-adapted (F_{NPQ}; PSII RCs closed) state. Although the unquenched decays were similar for all gen-

TABLE 1

Average fluorescence lifetimes τ_{av}(ps) at 686 nm

The maximum error in average lifetimes is ±5%, the maximum error in the *NPQ* (τ_{av}) values is ±10%.

	WT	koCP26	koCP24/CP26	koCP29
F_0	210	193	394	315
F_{NPQ}	410	302	336	460
F_m	1230	917	991	1376
$NPQ\ (\tau_{av})^a = (\tau_{av}\ (F_m)/\tau_{av}\ (F_{NPQ})) - 1$	2.0	2.0	1.9	2.0

[a] This NPQ value corresponds to the NPQ value determined from steady state fluorescence intensity by the PAM instrument.

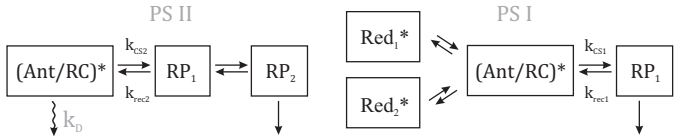

FIGURE 3. **Kinetic schemes for PSI and PSII used in the global target analysis of the fluorescence decays from *A. thaliana* leaves.** Where necessary additional single lifetime components were allowed in the analysis (see *e.g.* Figs. 5 and 6 and supplemental Fig. S1) to describe antenna components detached from the PSII supercomplex. These additional lifetimes represent either newly appearing components that could not be fitted within the above pure PSI and PSII schemes and/or for some mutants PSII antenna components that were already present in the dark-adapted state. Such component(s) are needed to describe functionally detached LHCII. k_{CS}, rate constant of charge separation reaction; k_{rec}, rate constant of charge recombination; k_D, rate constant for energy dissipation by non-radiative decay and non-photochemical quenching (32).

otypes in particular in the short time range, but showing some differences in the long time range (see below), the decays for quenched conditions showed large differences in overall kinetics. Table 1 summarizes the average lifetimes for each decay and the NPQ values calculated from the lifetime data at the 686 nm emission wavelength. All genotypes showed a ~3-fold shortening of the average lifetime under quenching conditions. From the average lifetimes the NPQ value can be calculated (Table 1). This NPQ value should be close to the values obtained by the steady state PAM measurements (note, however, that some differences are expected to arise between the two types of measurement because in the typical PAM measurement detection occurs in a different wavelength range, which contains a large contribution of PSI fluorescence, whereas at 686 nm (Fig. 1) essentially only PSII fluorescence contributes (33)). The lifetime-based NPQ values were for almost all mutants and the WT in a narrow range (around 2.0). Besides kinetics at F_m and F_{NPQ}, fluorescence decay kinetics were also measured at F_0 to detect possible disconnections of antenna proteins in the dark-adapted state resulting from the absence of monomeric Lhcb proteins that, in WT, connect the PSII core complex to the outer antenna system (2). The results are shown in supplemental Fig. S1. The decays for F_0 conditions showed strong differences in particular in the longer time range. Comparison based on the average lifetimes shows that the slowest kinetics was observed for koCP24/CP26 (τ = 394 ps). koCP29 kinetics was slightly faster (τ = 315 ps), whereas the fastest average lifetime was observed for both koCP26 and WT (τ = 193 and 210 ps, respectively). The results show clearly that the longer F_0 average lifetimes are due to the presence of variable amounts of loosely connected peripheral antenna complexes in some of the mutants. These results are in full agreement with the results of a previous lifetime study carried out under F_0 conditions on isolated chloroplasts of the same mutants that were used to study the influence of varying functional PSII antenna size on the energy trapping kinetics (43).

Target Compartment Modeling—For a deeper insight into the origin of the lifetime components, the fluorescence decays were submitted to global target analysis. The rate constants of the kinetic schemes shown in Fig. 3 were fitted to the experimental data that allowed for dissection of PSI and PSII kinetics in the fluorescence decay (32). These kinetic models for PSI and PSII are based on previous results from time-resolved measurements and fluorescence lifetime analysis of isolated PSI (44) and PSII particles (45–49) of vascular plants and cyanobacteria. The adequacy of these models has been discussed extensively by Holzwarth *et al.* (32). The kinetic scheme results in a number of rate constants reflecting energy and electron transfer processes. The PSII scheme has one excited state compartment of antenna/RC and two radical pairs (RPs), which account for reductions of pheophytin (RP1) and plastoquinone Q_A (RP2). PSI is described by one excited state compartment of antenna and RC, one RP and two "red" antenna compartments assigned to red-shifted long-wave Chls (44).

Detached Antenna Component—The compartment model in Fig. 3 was tested for both F_m and F_{NPQ} conditions. The resulting DAS for WT and all knockout mutants are shown in Figs. 4 and 5, for F_m and F_{NPQ} conditions, respectively. These kinetic schemes with three PSII and four PSI compartments (Fig. 3) resulted in a very good fit of the kinetics for the dark-adapted unquenched WT and koCP26 conditions across the whole wavelength range (Fig. 4), whereas the other mutants required an additional long-lived lifetime component(s) accounting for the detached antenna complement in the dark-adapted state (43). The largest differences between the unquenched and the HL-adapted quenched conditions were: (i) the average lifetimes in the quenching condition were two to three times shorter compared with the unquenched condition, as expected based on the steady state NPQ analysis, and (ii) an additional lifetime component beyond the scheme shown in Fig. 3, marked in *red* in Fig. 5, was required for a good fit under quenching conditions. This additional short lifetime component reflects a strongly quenched antenna component that is functionally disconnected from both PSI and PSII. Without such an additional component the data for the quenched condition for all genotypes could not be fitted well. This is reminiscent of the observations under quenching conditions observed previously for WT and other mutants (32). The shape of the fluorescence spectrum (DAS) of this additional component is quite different from the components of PSI and PSII. The peak of its emission spectrum is slightly red-shifted as compared with the normal PSII emission and it shows enhanced emission in the long-wavelength range, appearing as a broad plateau above 700 nm, relative to the "normal" PSII spectra shown in Fig. 4.

Quantitative Analysis of the Detached Antenna Component—Under the HL condition (F_{NPQ}), the mutations affected strongly both the lifetime of the additional "detached antenna" compartment (Q1 site) and the percentage of antenna detachment, which was strongly dependent on the presence/absence of specific monomeric CP complexes. For a quantitative com-

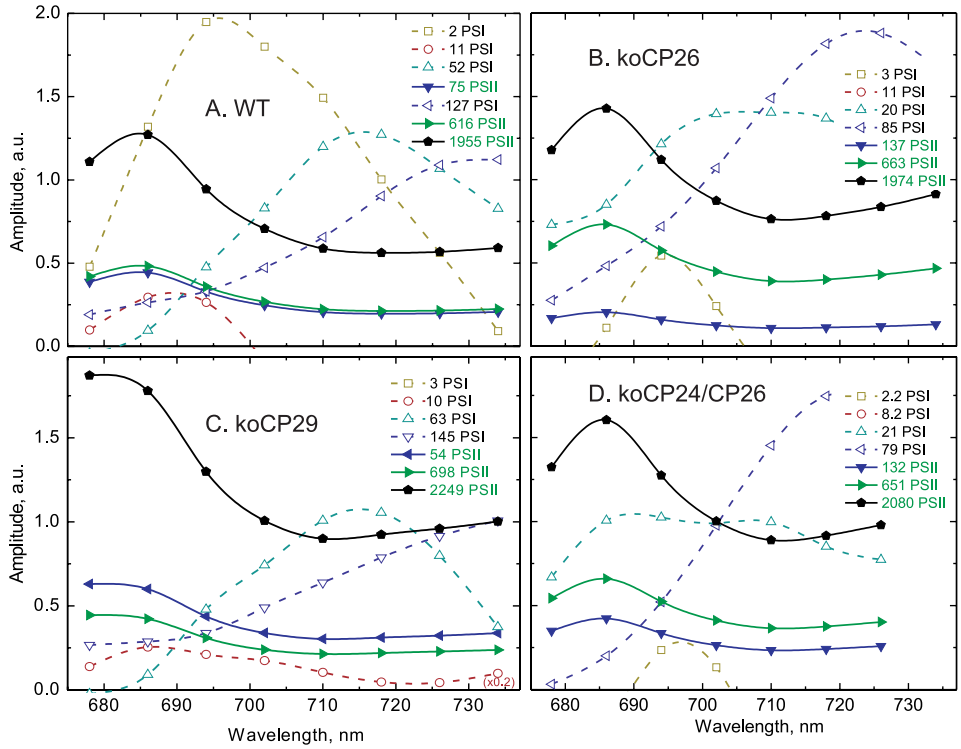

FIGURE 4. **Fluorescence lifetime components (recalculated DAS) of dark-adapted plants resulting from global target analysis of the fluorescence decays of leaves from WT (*A*) and knockout mutants koCP26 (*B*), koCP24/CP26 (*D*), and koCP29 (*C*) under unquenched (F_m) conditions.**

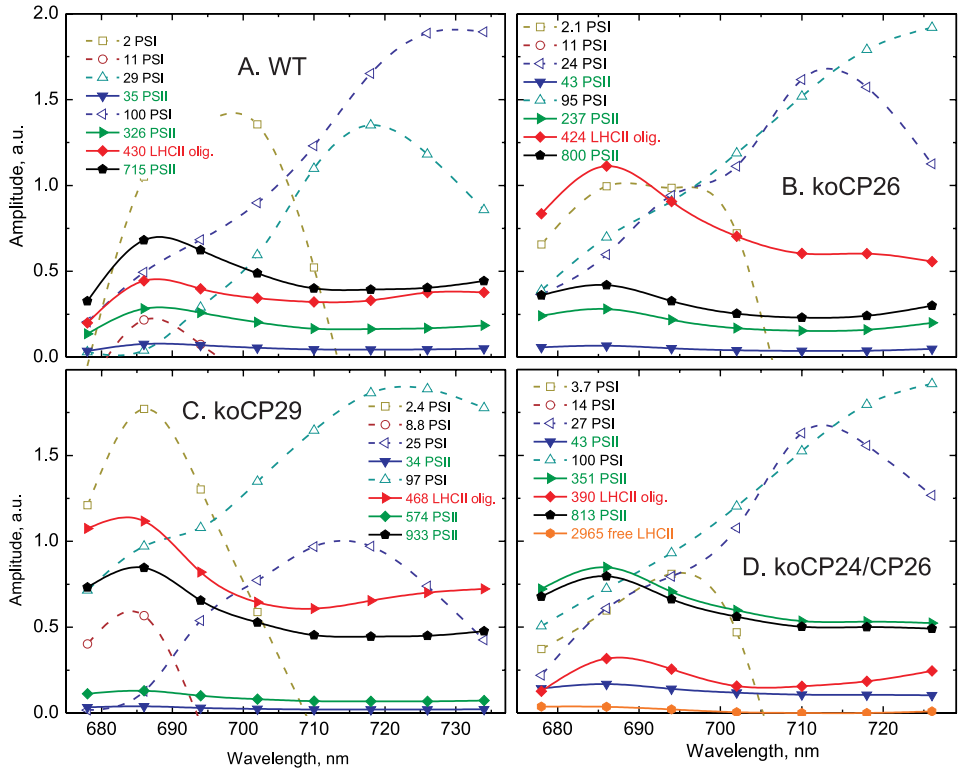

FIGURE 5. **Fluorescence lifetime components (recalculated DAS) of high light-adapted plants resulting from global target analysis of the fluorescence decays of leaves from WT (*A*) and knockout mutants koCP26 (*B*), koCP24/CP26 (*D*), and koCP29 (*C*) under quenched (F_{NPQ}) conditions.**

parison, the DAS amplitude of the detached LHCII component at its fluorescence maximum (686 nm) was calculated relative to the total amplitude of PSII plus detached LHCII components. This value is given as "percentage of detached PSII antenna" in Table 2. Concomitant with the appearance of the detached antenna component, the relative total DAS amplitude of the PSII lifetime components decreased. Thus, this additional fluorescence decay component originates from an

TABLE 2

Parameters of detached antenna components

Lifetime τ (ps) of the additional compartment assigned to quenched LHCII oligomers, percentage of detached LHCII, the average number of associated Chl *a* molecules, and the corresponding number of detached LHCII trimers. The maximum error in the lifetime of the detached antenna compartment is ±10%, the error in percentage of detached antenna is also ±10%. The data are averaged over measurements on 30–40 leaves.

	WT	koCP26	koCP24/CP26	koCP29
t [ps] of detached LHCII/CPxx compartment	430	424	390	468
Percentage of detached PSII antenna[a]	30	59	15	52
Equivalent number of Chl *a* molecules in detached PSII antenna[b]	69	134	26	93
Equivalent number of detached LHCII trimers[c]	2.8	5.6	1.1	3.9

[a] Calculated from the amplitude of the detached PSII antenna component in the DAS at its fluorescence maximum (686 nm) relatively to the total (sum of the amplitudes of the three PSII components + amplitude of detached antenna component) (32).

[b] The number of Chl *a* molecules corresponding to the percentage of detached LHCII/CP. This value was calculated relative to the total Chl *a* per PSII supercomplex, which was assumed to be $C_2S_2M_2$ in WT and koCP26; $C_2S_2M_2$ in koCP29 and C_2S_2M in koCP24/CP26 in the darkness (see text).

[c] The number of LHCII trimers that corresponds to the calculated number of Chl *a* in the detached PSII antenna. The composition of PSII antenna compartment and detached antenna compartments shown in Fig. 6 reflects this number.

TABLE 3

Parameters of PSII and attached antenna complexes

Average lifetimes τ_{av} of the pure PSII compartment (as obtained from global target analysis). The value of NPQ in the Q2 site is calculated from the τ_{av} of the pure PSII components rather than the total fluorescence at 686 nm (Table 1), the non-photochemical deactivation rates k_D, ns^{-1} of the PSII complex under dark-adapted (F_m) and NPQ conditions (F_{NPQ}), and the NPQ value calculated from the PSII antenna deactivation rates k_D. The error in k_D is ±5% and in $NPQ^{(Q2)}$ ±10%. The data are averaged over measurements on 30–40 leaves.

Pure PSII parameters	WT	koCP26	koCP24/CP26	koCP29
τ_{av} (ps), F_{NPQ}	560	528	525	852
τ_{av} (ps), F_{max}	1280	1409	1422	1544
$NPQ^{(Q2)}$ from τ_{av}	1.3	1.7	1.7	0.8
k_D, ns^{-1}, F_{NPQ}	1.7	1.7	1.7	1.1
k_D, ns^{-1}, F_{max}	0.4	0.3	0.3	0.3
$NPQ^{(Q2)} = (k_D^{(NPQ)}/k_D^{(Fm)}) - 1$	3.3	4.1	4.0	2.8

antenna compartment that becomes disconnected functionally from PSII in the light and thus decreases the total PSII cross-section. Due to the high percentage of PSII antenna detachment (corresponding to up to 60% of the initial total PSII antenna amplitude in the dark) this component predominantly must reflect a part of LHCII that becomes detached from PSII during the onset of NPQ, because LHCII accounts for approximately 70% of the total Chl content of PSII (32). The lifetime of the detached antenna component varied between 390 and 470 ps, implying that it is strongly quenched as compared with the PSII antenna of dark-adapted leaves under F_m conditions whose lifetime is 1.23 ns (Table 1). This lifetime component, which is very short-lived with respect to that of isolated trimeric LHCII (25) corresponds to the Q1 quenching site (32).

Because the DAS amplitude is approximately proportional to the absorption cross-section of the excited pigments at 668 nm, *i.e.* Chl *a* in our case, the relative amplitude percentage of the detached antenna is proportional to the number of Chl *a* molecules (or equivalent number of LHCII trimers, *i.e.* 24 Chl *a*) detached per PSII supercomplex (Table 2). Note that we use the term "trimer" in this situation only formally, irrespective of the possibility that a certain amount of LHCII monomers may also be detached or be present instead of trimers only. Our methods do not allow for a distinction of these two cases. For this calculation we assume that PSII in the dark-adapted state is organized as $C_2S_2M_2L$ supercomplexes in WT containing 230 Chl *a* molecules (2 PSII cores + 2 copies of CP24, CP26, CP29 + 5 LHCII trimers) based on the experimental stoichiometric analysis of antenna proteins (50). In the knockout mutants part of the missing complexes are compensated by overaccumulation of other Lhc subunits (30) as shown by the measurement of functional antenna size, which yields values not statistically distinguishable from WT. For koCP29 we assume a $C_2S_2M_2$ organization and for CP24/CP26 a C_2S_2M, on the basis of the electron microscopy analysis (30, 51, 52).

In the koCP24/CP26 mutant a very small amount of one further antenna compartment, also not connected to either PSI or PSII, was necessary to fit the data (Fig. 5*D,* labeled *free LHCII*). Its lifetime is very long (3 ns) and the relative amplitude of its emission spectrum was <5%. We assign it to a small number of free LHCII trimers that are functionally disconnected from the photosystems due to the large distance between PSII core complexes and antenna-only domains in this double mutant (30). This component does not undergo quenching under HL conditions (Fig. 5*D*). It is very likely that this small amount of LHCII detachment is already present in the dark-adapted state of the double mutant, which is actually supported by the small amount of long-lived (ns lifetime) components present also in the dark-adapted F_0 condition (*cf.* Fig. 2). This leads to an increased τ_{av} and F_0 value (Table 1). Similar small components are also present in the other monomeric CP knockout mutants because they also show some increased τ_{av} and F_0 value. However, they do not show an unquenched long lifetime component under HL conditions. This suggests that in these other mutants the antenna part detached already in the dark becomes quenched under HL conditions.

Non-photochemical Deactivation Rate Constant k_D for PSII Compartment—Within the PSII model (Fig. 3) the most important rate constant, which directly characterizes the quenching in the PSII-connected antenna is k_D. It represents the effective total non-photochemical deactivation rate of the PSII complex. Table 3 compares the k_D values for quenched and unquenched leaves (k_D, F_{NPQ}; k_D, F_{max}). These values allow us to calculate the specific NPQ value for the PSII-attached antenna part according to the Stern-Volmer equation (53). We will refer to this PSII-connected antenna quenching as the "Q2 quenching

site" (32). This Q2-related *NPQ* is denoted as $NPQ^{(Q2)}$ to avoid confusion with the overall *NPQ* value obtained from PAM measurements and from the average fluorescence lifetime measurements (Table 1). koCP26 and koCP24/CP26 show slightly higher values of $NPQ^{(Q2)}$ than WT (1.7 *versus* 1.3), however, koCP29 shows a $NPQ^{(Q2)}$ that is decreased by 50–60%, indicating strongly impaired quenching.

DISCUSSION

Before interpreting in detail the results from these knockout mutants, it was necessary to verify that lack of minor antennae did not induce major pleiotropic effects that could influence the heat dissipation properties of the genotypes by affecting general parameters of the photosynthetic function rather than specifically the NPQ machinery. We thus performed a detailed analysis of PSII functional antenna size, efficiency of linear electron transport, extent of excitation pressure on PSII, and capacity for building trans-thylakoid ΔpH on WT and knockout mutant plants. Results are summarized in supplemental Table S1. We found no restriction in electron transport rates in koCP26, koCP29, and koCP24/CP26 with respect to WT, as well as no significant alteration in PSII functional antenna size and the extent of ΔpH formation across the thylakoid membrane. These results imply that all mutations investigated do not negatively affect the functioning of neither the photosynthetic machinery nor the main parameters that modulate the chlorophyll fluorescence quenching *in vivo*. On this basis we consider it safe to proceed to the interpretation of the quenching phenotype observed on the basis of the presence/lack of specific light-harvesting complexes and their consequent effect on the organization of PSII supercomplexes within the grana membranes and its dynamics during NPQ onset (31).

Two Quenching Sites—In general the lifetime and target analysis of the fluorescence decays for all the monomeric CP knockout mutants presented here support the model of two different non-photochemical quenching sites under HL adaptation. These two sites are (*a*) the Q1 site reflecting the functional detachment of part of the antenna of the PSII supercomplex, and (*b*) the Q2 quenching site that is located in the antenna that remains attached to the PSII core under HL conditions. The functional antenna detachment follows from the decrease of the PSII lifetime amplitude and the concomitant appearance of a new "detached antenna compartment" upon HL adaptation for all the monomeric CP knockout mutants. Specifically, the lifetime of the detached antenna (Q1 site) in the range of 390–470 ps under HL conditions *in vivo* (25) is much shorter than the lifetime of isolated LHCII antenna complexes (Ref. 54, ~3–4 ns) or the average PSII lifetime in dark-adapted unquenched leaves with closed RC (1.3–1.4 ns) (Table 1, *cf.* also Ref. 32). This indicates that a special quenching mechanism is active in this site. It has been demonstrated before that the functional antenna detachment occurs only if PsbS is activated and the quenching mechanism for the most part does not require Zx (32). In the PsbS-lacking mutant, *npq4,* there was no formation of a new detached antenna compartment with spectral and kinetic properties of a far-red emitting and quenched LHCII antenna. These spectroscopic evidences are consistent with the finding that in the WT, PsbS, upon protonation by low lumenal pH, causes a dissociation of the B4 complex, composed of CP29, CP24, and LHCII-M. This eventually leads to the segregation of the dark-adapted PSII supercomplex into two domains, one including PSII core, CP29 and CP26 (C_2S_2 complex), and a second domain containing CP24 together with LHCII-M and LHCII-L (31). The high percentage of PSII antenna detachment (up to 60% in some cases) is only consistent with an interpretation where the detached antenna consists primarily of LHCII (31, 32). We assume that LHCII-M trimers are easier to detach than LHCII-S trimers because they are less strongly connected to PSII (55, 56) and because they belong to the "B4" supercomplex dissociated during NPQ (31). Because the level of PsbS is not affected in knockout mutants of the monomeric Lhcbs (30), we expect partial antenna detachment and activation of the Q1 quenching site under HL unless the quencher is the knocked-out monomeric Lhcb complex targeted by the mutation. On this basis, the main part of the quenching of the detached LHCII antenna (quenching from about 4.1 ns (25) down to about 490 ps) does not strongly depend on the presence of monomeric Lhcb complexes, notably of CP24, which partitions out of the C_2S_2 supercomplexes during NPQ-dependent segregation of PSII subunits (31).

The quenching mechanism active in the PSII-attached antenna (Q2) increases the deactivation rate k_D, which is a direct fitting parameter of the model, thus allowing for a direct measurement of the PSII-related quenching effect (Fig. 3, see also Ref. 32). This cannot be obtained by steady state PAM measurements. This quenching has been shown to be strictly dependent on the presence of Zx (32). Because the Q2 mechanism directly quenches the antenna functionally attached to PSII, it should be centered in the monomeric antenna complexes; indeed, according to Bassi *et al.* (57), 80% of the xanthophyll-cycle active carotenoids is located in the monomeric CP complexes.

The present results strongly support the model for the mechanism of non-photochemical quenching recently proposed on the basis of independent functional and structural measurements (31, 32), which suggested the structural and functional compartmentalization of the components of PSII, a single large supramolecular complex stable under LL conditions, into two distinct domains upon exposure to excess light. Domain A consists of the PSII core complex in its C_2S_2 configuration, which includes the monomeric antenna CP29 and CP26 and the LHCII-S trimer. Domain B consists of LHCII-M and -L trimers plus CP24 (31). Here we show that quenching in domain A corresponds to the previously proposed Q1 site, whereas domain B corresponds to the proposed Q2 site (32). The presence of certain minor CP complexes is crucial for the quenching in that site. Notably the occurrence of two quenching sites in WT and the monomeric CP knockout mutants of higher plants is also in agreement with the recent findings of two equivalent quenching sites contributing to total NPQ in diatoms, *i.e. Phaeodactylum tricornutum* and *Cyclotella meneghiniana* (58).

In the following, we discuss the specific roles exerted by the various monomeric CP complexes on the appearance and regulation of total NPQ at these two quenching sites. By knocking out these complexes one by one, we may expect to gain detailed insight into the regulation and location of the specific quench-

ing mechanisms and the roles of the monomeric CP complexes. The analysis and interpretation of the experimental findings is, however, somewhat complicated by the fact that knockout of some of the monomeric complexes has some side effects, like *e.g.* co-suppression and/or compensatory overexpression of other Lhcb complexes.

A strong decrease of the k_D constant of site Q2 is observed in koCP29, consistent with its localization in the C_2S_2 particles upon segregation of PSII antenna under quenched conditions (31). Interestingly, koCP26 does not show any reduction in Q2 quenching efficiency *versus* WT, implying that CP29 is the major site for Q2 quenching. Rather, k_D for Q2 is even increased in koCP26 (comparing to WT), which can be well understood based on the compensatory increase in CP29 content in the koCP26 mutant (30).

The NPQ Quenching Model and the Role of the Monomeric CP Complexes—From the fluorescence kinetics data we can now construct a model describing the parallel action of the Q1 and Q2 quenching sites and the specific role of the monomeric CP complexes in these sites, which includes their function in the HL-induced reorganizations of PSII in the thylakoid membrane. This discussion is based on the finding that *Arabidopsis* WT, as well as koCP26, have a $C_2S_2M_2$ type of PSII supercomplex organization in the darkness (55, 56), whereas other mutants, lacking CP24 protein, have C_2S_2, C_2S_2M, or $C_2S_2M_2$ organization, respectively (29, 30). In koCP24/CP26 and koCP29, LHCII-M (Fig. 6) is present in the dark-adapted state but is not connected to the core with the same strength as in WT, due to the loss of the connecting monomeric Lhcb subunits.

In WT both quenching sites, Q1 and Q2, are active. The fraction of PSII antenna detached under HL conditions is 30%, corresponding on average to two to three LHCII trimers per PSII supercomplex, based on the Chl *a* content (Table 2). Because loosely (-L) and moderately (-M) bound LHCII complexes are supposed to detach easier than strongly bound ones (LHCII-S), we propose that the prevailing part of PSII supercomplexes in WT is organized as C_2S_2 type under HL conditions (Fig. 6).

The koCP26 mutant also possesses two quenching sites. About double the amount of LHCII trimers detach from PSII in this mutant forming the Q1 quenching site under HL. Taking the Chl *a* content into consideration, this corresponds to 5–6 detached LHCII trimers per PSII supercomplex, which implies the detachment of all LHCII trimers. Because the percentage of antenna detachment in koCP26 is larger than in WT, and because the $NPQ^{(Q2)}$ at the Q2 site is also higher than in WT (1.7 *versus* 1.3), we can conclude that the CP26 complex is less important than CP29 for the generation of NPQ. Apparently CP26 has no major direct role in quenching, when CP29 is present in the PSII supercomplex as in WT. Nevertheless, in the absence of CP29, Q2 quenching is still active, although to a lower extent, whereas a fraction of the LHCII-S complement in these mutants becomes detached, suggesting a quenching role for CP26. This conclusion is in agreement with a previous finding of sustained quenching associated to this protein subunit (34). Besides, it plays an important role for supercomplex integrity. We thus suggest that in CP26 the absence of binding cooperativity of LHCII to the PSII core is disturbed and that dissociation of the B4 complex induces detachment not only of LHCII-M and -L but LHCII-S as well (in accordance with Ref. 2).

Interestingly the koCP24/CP26 mutant is able to generate as efficient quenching in the Q2 site as koCP26 and WT despite a different structure in darkness. Apart from the absence of CP24 and CP26, this mutant has a ~25 and ~50% reduced content of CP29 and Lhcb3, respectively (30), which is compensated by increased amounts of Lhcb1 (60%) and Lhcb2 (10%). We hypothesize hence that the empty sites of CP24 and CP26 are occupied by Lhcb1 and Lhcb2 complexes that become involved in the Q2 site of quenching possibly via Lhcb-Lhcb or Lhcb-CP29 interactions (Fig. 6). At the Q1 site the detached amount of LHCII is strongly decreased. The related presence of some free LHCII complexes that are not quenched under HL conditions indicates some disturbance in the supercomplex organization in this double mutant, which is already evident in the dark-adapted state (see above). This interpretation of the lifetime data is also supported by electron microscopy measurements (30), which show regions of LHCIIs with rows of connected PSII cores in grana membrane disks.

The koCP29 mutant is lacking not only CP29 but also CP24, thus actually representing a phenocopy of a koCP24/CP29 plant. This lack of CP24 is compensated by an increase in Lhcb1 content by about 40% (52). The antenna detachment yielding the Q1 site is very strong in this mutant (Table 2), equivalent to four LHCII trimers per supercomplex. Despite the absence of CP29 the Q2 site is still active, although to a lower extent. This may hint to some quenching contribution by CP26. Under HL conditions the nominal k_D is ~43% of the WT value for the koCP29 mutant. This demonstrates on the one hand the crucial role of CP29 in Q2 site quenching, but also indicates that CP29 can apparently be replaced in its quenching function to some extent by CP26. Within the monomeric Lhcb subfamily, CP26 occupies an intermediate position between CP29 and CP24 for many biochemical and spectroscopic properties (59–61) and it has also been shown to be active in radical cation quenching (20). We thus propose that CP26 can substitute partially for CP29 in Q2 quenching in C_2S_2 supercomplexes. It is clear, however, that Lhcb1 cannot structurally replace CP29 in the C_2S_2 supercomplex as follows from the results of the recent electron microscopy study (52) (*cf.* Fig. 6).

As far as the Q1 quenching is concerned, the lifetime of the detached antenna compartment in the knockout mutants is similar to the WT (~400 ps). This implies that monomeric Lhcbs are not absolutely required. This conclusion is, however, contrasting with the longer lifetime observed for koCP24 in isolated thylakoids (43) and with the enhanced quenching of LHCII provided by addition of CP24 in an *in vitro* system (62). It is possible that the increased level of LHCII detachment induced by the deletion of monomeric Lhcbs, particularly in koCP26/CP24 might increase quenching and compensate for the missing CP24 with respect to WT. From various studies a Chl-Chl charge transfer mechanism of quenching has been proposed for the Q1 site located within the LHCII complexes alone without requiring interaction with monomeric CP complexes (24, 25, 32, 33). Alternatively at least some part of the

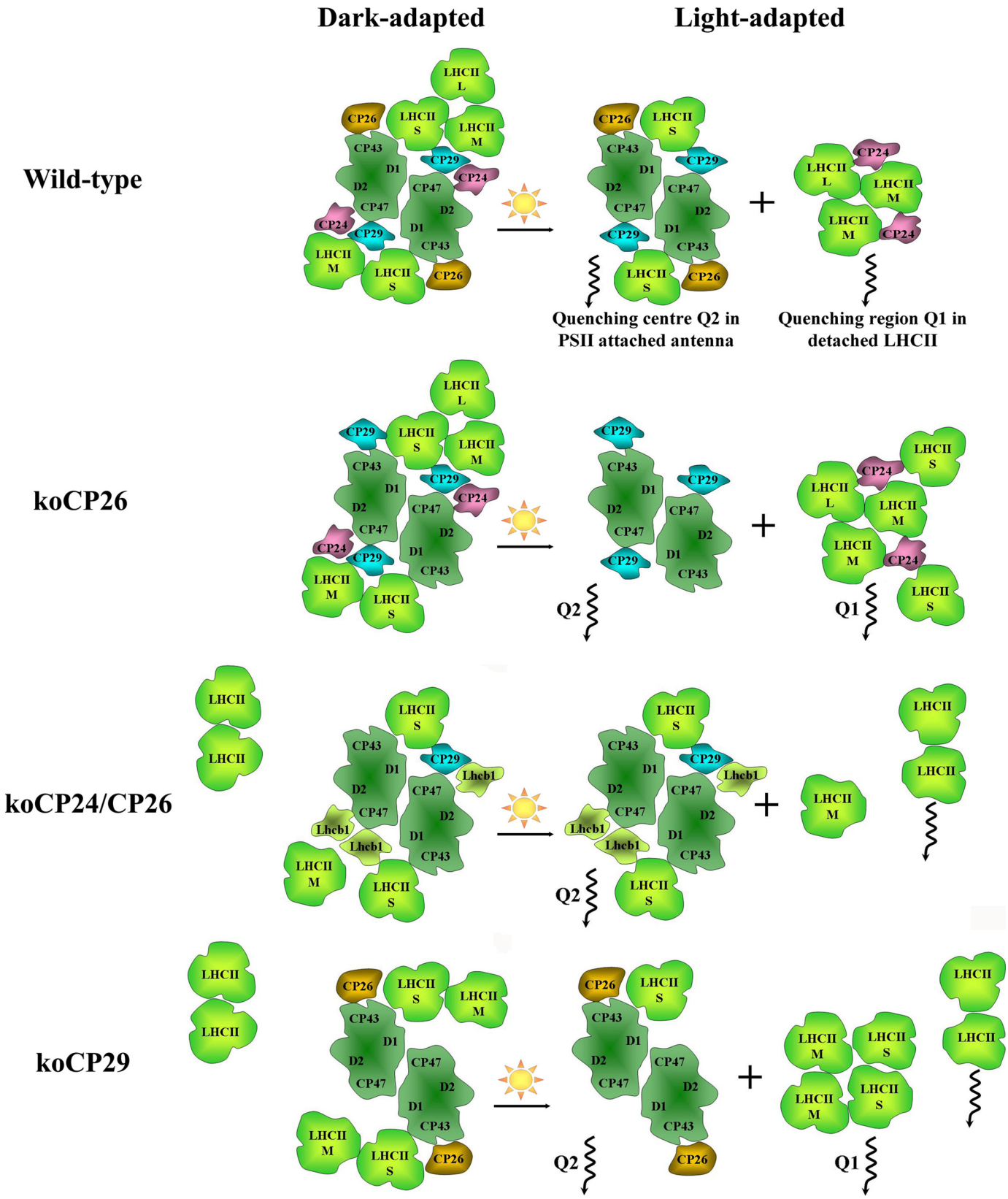

FIGURE 6. **Model of the PSII supercomplex reorganization under high light adaptation.** *S*, *M*, and *L* denote strongly, moderately, and loosely bound LHCII, respectively. The composition of the dark-adapted antennae (*left hand side*) is based on the respective electron microscopy works (30, 51, 55, 56) and the amount of detached LHCII antenna is based on the amplitude of long-lived 2–3-ns components in the dark-adapted fluorescence. The degree of the antenna detachment under high-light conditions is based on the percentage (relative amplitude) of the detached antenna component in relationship to the total PSII antenna (amplitude of PSII attached + detached antenna components).

CP24 quenching function could, for example, be functionally compensated by CP29, which in this mutant is accumulated in excess with respect to the 1:1 stoichiometry with PSII and binds ectopically to the C_2S_2 supercomplex (30). This hypothesis might be consistent with the activity of CP29 in charge-transfer quenching (26), and with the ability of minor antenna complexes, as shown for CP26, to interact with LHCII-S (2) even forming trimeric structures in the absence of LHCII (63). A more definitive answer to this question may probably be provided by specific Zx deletion and monomeric CP knockout double mutants.

Conclusions—The present study strongly supports and details the previously proposed model of two quenching sites active in *Arabidopsis* leaves under HL. The results provide specific insight into the complex role of the monomeric CP complexes for both the quenching itself as well as their role in the thylakoid reorganization related to NPQ as a whole. One quenching site, Q1, is formed by a PsbS-dependent detachment of peripheral antenna, mostly LHCII trimers, from PSII. The most effective quenching mechanism in this Q1 site is very likely a Chl-Chl charge transfer mechanism located in the major LHCII complexes, which does not involve carotenoids and does, in particular, not require Zx (25, 32, 33). The second quenching site Q2 is located in the PSII-attached antenna and quenching strictly depends on Zx and was proposed to be located primarily in the various monomeric Lhcb complexes (32). The present results demonstrate that CP29 is the most crucial complex for Q2 quenching in the WT situation. However, none of the three Lhcbs is indispensably required for the Q2 mechanism to take place because CP26 can, at least partially, take over the quenching function of CP29 in the Q2 site. Zx-activated nonradiative dissipation processes have been shown to occur in all of these monomeric CP complexes (20, 21). Thus there exists no complete specificity among the monomeric complexes with respect to quenching in the two sites, but there exists a specificity regarding the functional assembly and organization of the PSII supercomplex and the arrangement of PSII in the membrane. This organization can affect the energy and electron transport processes and hence, indirectly, NPQ. Thus, the location of LHCII subunits and the interactions with the neighboring complexes is at least as important for NPQ as the intrinsic properties of the monomeric CP complexes themselves. If one antenna complex is missing, others can in part take over the role of that missing Lhcb complex. This exemplifies the high flexibility of the photosynthetic apparatus with regards to its ability to reorganize and maintain both a functional and also a photoprotected structure of PSII.

REFERENCES

1. Ben-Shem, A., Frolow, F., and Nelson, N. (2003) *Nature* **426,** 630–635
2. Caffarri, S., Kouril, R., Kereïche, S., Boekema, E. J., and Croce, R. (2009) *EMBO J.* **28,** 3052–3063
3. Holzwarth, A. R. (2008) in *Ultrashort Laser Pulses in Biology and Medicine* (Braun, M., Gilch, P., and Zinth, W., eds) pp. 141–164, Springer, Dordrecht
4. Holzwarth, A. R. (2004) in *Molecular to Global Photosynthesis* (Archer, M. D., and Barber, J., eds) pp. 43–115, Imperial College Press, London
5. Müller, P., Li, X. P., and Niyogi, K. K. (2001) *Plant Physiol.* **125,** 1558–1566
6. de Bianchi, S., Ballottari, M., Dall'osto, L., and Bassi, R. (2010) *Biochem. Soc. Trans.* **38,** 651–660
7. Horton, P. (1996) in *Light as an Energy Source and Information Carrier in Plant Physiology* (Jennings, R. C., ed) pp. 99–111, New York, Plenum Press
8. Niyogi, K. K. (1999) *Annu. Rev. Plant Physiol. Plant Mol. Biol.* **50,** 333–359
9. Yamamoto, H. Y., and Kamite, L. (1972) *Biochim. Biophys. Acta* **267,** 538–543
10. Demmig-Adams, B. (1990) *Biochim. Biophys. Acta* **1020,** 1–24
11. Demmig-Adams, B., Winter, K., Kruger, A., and Czygan, F. C. (1989) in *Photosynthesis, Plant Biology* (Briggs, W. R., ed) Vol. 8, pp. 375–391, Alan R. Liss, New York
12. Li, X. P., Gilmore, A. M., Caffarri, S., Bassi, R., Golan, T., Kramer, D., and Niyogi, K. K. (2004) *J. Biol. Chem.* **279,** 22866–22874
13. Li, X. P., Muller-Moule, P., Gilmore, A. M., and Niyogi, K. K. (2002) *Proc. Natl. Acad. Sci. U.S.A.* **99,** 15222–15227
14. Bonente, G., Howes, B. D., Caffarri, S., Smulevich, G., and Bassi, R. (2008) *J. Biol. Chem.* **283,** 8434–8445
15. Briantais, J. M. (1994) *Photosynth. Res.* **40,** 287–294
16. Havaux, M., Dall'osto, L., and Bassi, R. (2007) *Plant Physiol.* **145,** 1506–1520
17. Jansson, S. (1994) *Biochim. Biophys. Acta* **1184,** 1–19
18. Jackowski, G., and Jansson, S. (1998) *Z. Naturforsch. C* **53,** 841–848
19. Ruban, A. V., Berera, R., Ilioaia, C., van Stokkum, I. H., Kennis, J. T., Pascal, A. A., van Amerongen, H., Robert, B., Horton, P., and van Grondelle, R. (2007) *Nature* **450,** 575–578
20. Ahn, T. K., Avenson, T. J., Ballottari, M., Cheng, Y. C., Niyogi, K. K., Bassi, R., and Fleming, G. R. (2008) *Science* **320,** 794–797
21. Avenson, T. J., Ahn, T. K., Zigmantas, D., Niyogi, K. K., Li, Z., Ballottari, M., Bassi, R., and Fleming, G. R. (2008) *J. Biol. Chem.* **283,** 3550–3558
22. Cheng, Y. C., Ahn, T. K., Avenson, T. J., Zigmantas, D., Niyogi, K. K., Ballottari, M., Bassi, R., and Fleming, G. R. (2008) *J. Phys. Chem. B* **112,** 13418–13423
23. Holt, N. E., Zigmantas, D., Valkunas, L., Li, X. P., Niyogi, K. K., and Fleming, G. R. (2005) *Science* **307,** 433–436
24. Müller, M. G., Lambrev, P., Reus, M., Wientjes, E., Croce, R., and Holzwarth, A. R. (2010) *Chem. Phys. Chem.* **11,** 1289–1296
25. Miloslavina, Y., Wehner, A., Lambrev, P. H., Wientjes, E., Reus, M., Garab, G., Croce, R., and Holzwarth, A. R. (2008) *FEBS Lett.* **582,** 3625–3631
26. Avenson, T. J., Ahn, T. K., Niyogi, K. K., Ballottari, M., Bassi, R., and Fleming, G. R. (2009) *J. Biol. Chem.* **284,** 2830–2835
27. Li, Z., Ahn, T. K., Avenson, T. J., Ballottari, M., Cruz, J. A., Kramer, D. M., Bassi, R., Fleming, G. R., Keasling, J. D., and Niyogi, K. K. (2009) *Plant Cell* **21,** 1798–1812
28. Andersson, J., Walters, R. G., Horton, P., and Jansson, S. (2001) *Plant Cell* **13,** 1193–1204
29. Kovács, L., Damkjaer, J., Kereïche, S., Ilioaia, C., Ruban, A. V., Boekema, E. J., Jansson, S., and Horton, P. (2006) *Plant Cell* **18,** 3106–3120
30. de Bianchi, S., Dall'Osto, L., Tognon, G., Morosinotto, T., and Bassi, R. (2008) *Plant Cell* **20,** 1012–1028
31. Betterle, N., Ballottari, M., Zorzan, S., de Bianchi, S., Cazzaniga, S., Dall'osto, L., Morosinotto, T., and Bassi, R. (2009) *J. Biol. Chem.* **284,** 15255–15266
32. Holzwarth, A. R., Miloslavina, Y., Nilkens, M., and Jahns, P. (2009) *Chem. Phys. Lett.* **483,** 262–267
33. Lambrev, P. H., Nilkens, M., Miloslavina, Y., Jahns, P., and Holzwarth, A. R. (2010) *Plant Physiol.* **152,** 1611–1624
34. Dall'Osto, L., Caffarri, S., and Bassi, R. (2005) *Plant Cell* **17,** 1217–1232
35. Van Kooten, O., and Snel, J. F. (1990) *Photosynth. Res.* **25,** 147–150
36. Walters, R. G., and Horton, P. (1995) *Planta* **197,** 306–312
37. Malkin, S., Armond, P. A., Mooney, H. A., and Fork, D. C. (1981) *Plant Physiol.* **67,** 570–579
38. Johnson, G. N., Young, A. J., and Horton, P. (1994) *Planta* **194,** 550–556
39. Holzwarth, A. R., Müller, M. G., Niklas, J., and Lubitz, W. (2005) *J. Phys. Chem. B* **109,** 5903–5911
40. Müller, M. G., Griebenow, K., and Holzwarth, A. R. (1992) *Chem. Phys. Lett.* **199,** 465–469
41. Holzwarth, A. R. (1996) in *Biophysical Techniques in Photosynthesis, Advances in Photosynthesis Research* (Amesz, J., and Hoff, A. J., eds) pp. 75–92, Kluwer Academic Publishers, Dordrecht
42. Tóth, S. Z., Schansker, G., and Strasser, R. J. (2005) *Biochim. Biophys. Acta*

1708, 275–282
43. van Oort, B., Alberts, M., de Bianchi, S., Dall'Osto, L., Bassi, R., Trinkunas, G., Croce, R., and van Amerongen, H. (2010) *Biophys. J.* **98,** 922–931
44. Slavov, C., Ballottari, M., Morosinotto, T., Bassi, R., and Holzwarth, A. R. (2008) *Biophys. J.* **94,** 3601–3612
45. Szczepaniak, M., Sugiura, M., and Holzwarth, A. R. (2008) *Biochim. Biophys. Acta* **1777,** 1510–1517
46. Miloslavina, Y., Szczepaniak, M., Müller, M. G., Sander, J., Nowaczyk, M., Rögner, M., and Holzwarth, A. R. (2006) *Biochemistry* **45,** 2436–2442
47. Broess, K., Trinkunas, G., van Hoek, A., Croce, R., and van Amerongen, H. (2008) *Biochim. Biophys. Acta* **1777,** 404–409
48. Broess, K., Trinkunas, G., van der Weij-de Wit, C. D., Dekker, J. P., van Hoek, A., and van Amerongen, H. (2006) *Biophys. J.* **91,** 3776–3786
49. Szczepaniak, M., Sander, J., Nowaczyk, M., Müller, M. G., Rögner, M., and Holzwarth, A. R. (2009) *Biophys. J.* **96,** 621–631
50. Ballottari, M., Dall'Osto, L., Morosinotto, T., and Bassi, R. (2007) *J. Biol. Chem.* **282,** 8947–8958
51. Morosinotto, T., Bassi, R., Frigerio, S., Finazzi, G., Morris, E., and Barber, J. (2006) *FEBS J.* **273,** 4616–4630
52. de Bianchi, S., Betterle, N., Kouril, R., Cazzaniga, S., Boekema, E., Bassi, R., and Dall'Osto, L. (2011) *Plant Cell* **23,** 2659–2679
53. Krause, G. H., and Jahns, P. (2003) in *Light-Harvesting Antennas in Photosynthesis* (Green, B. R., and Parson, W. W., eds) pp. 373–399, Kluwer Academic Publishers, Dordrecht
54. Moya, I., Silvestri, M., Vallon, O., Cinque, G., and Bassi, R. (2001) *Biochemistry* **40,** 12552–12561
55. Dekker, J. P., and Boekema, E. J. (2005) *Biochim. Biophys. Acta* **1706,** 12–39
56. Yakushevska, A. E., Jensen, P. E., Keegstra, W., van Roon, H., Scheller, H. V., Boekema, E. J., and Dekker, J. P. (2001) *Eur. J. Biochem.* **268,** 6020–6028
57. Bassi, R., Pineau, B., Dainese, P., and Marquardt, J. (1993) *Eur. J. Biochem.* **212,** 297–303
58. Miloslavina, Y., Grouneva, I., Lambrev, P. H., Lepetit, B., Goss, R., Wilhelm, C., and Holzwarth, A. R. (2009) *Biochim. Biophys. Acta* **1787,** 1189–1197
59. Croce, R., Canino, G., Ros, F., and Bassi, R. (2002) *Biochemistry* **41,** 7334–7343
60. Dainese, P., Santini, C., Ghiretti-Magaldi, A., Marquardt, J., Tidu, V., Mauro, S., Bergantino, E., and Bassi, R. (1992) in *Research in Photosynthesis* (Murata, N., ed) Vol. II, pp. 13–20, Kluwer Academic Publishers, Dordrecht
61. Ballottari, M., Mozzo, M., Croce, R., Morosinotto, T., and Bassi, R. (2009) *J. Biol. Chem.* **284,** 8103–8113
62. Ballottari, M., Girardon, J., Betterle, N., Morosinotto, T., and Bassi, R. (2010) *J. Biol. Chem.* **285,** 28309–28321
63. Ruban, A. V., Wentworth, M., Yakushevska, A. E., Andersson, J., Lee, P. J., Keegstra, W., Dekker, J. P., Boekema, E. J., Jansson, S., and Horton, P. (2003) *Nature* **421,** 648–652